5 Hydraulic Properties of Roots

M.T. Tyree

Symbols

A_r	Surface area of root (m^{-2})
C	Concentration of solutes (osmolal)
$\overline{C}_s$	Average solute concentration between inside and outside of root
d	Diameter
D	Diffusion coefficient ($m^2\ s^{-1}$)
F_m	Mass flow of solution ($kg\ s^{-1}$)
H_r	Classical root hydraulic conductance ($kg\ s^{-1}\ MPa^{-1}$)
J_r	Mass flux density or F_m per unit root surface area ($kg\ s^{-1}\ m^{-2}$)
J_s	Solute flux density ($mol\ s^{-1}\ m^{-2}$)
K_r	Thermodynamic root hydraulic conductance ($kg\ s^{-1}\ MPa^{-1}$)
ln(2)	natural log of 2
L	Length (m)
L_r	Thermodynamic root hydraulic conductance per unit root surface area ($kg\ s^{-1}\ m^{-2}\ MPa^{-1}$)
P	Pressure (MPa)
P_s	Solute permeability
RT	Gas constant times Kelvin temperature (Mpa $osmolal^{-1}$)
T_p	Time constant for pressure relaxation (s)
V	Volume
T_{s1} and T_{s2}	Time constants for pressure relaxation after changing outside solute concentration

Ecological Studies, Vol. 168
H. de Kroon, E.J.W. Visser (Eds.)
Root Ecology
© Springer-Verlag Berlin Heidelberg 2003

α	Fraction of water root surface area occupied by water in apoplast
δ	Path length (m)
Δ	Difference
π	Osmotic potential (MPa) except in Eq. (5.8) where it denotes pi=3.14159...
Ψ	Water potential (MPa)
η	Viscosity of water
σ	Reflection coefficient

Subscripts: *i* inside; *o* outside; *r* root; *s* solute; *L* leaf; *sh* shoot

5.1 Introduction

The primary function of roots is to provide water and solute (primarily mineral ion) transport from the soil to the shoots of plants. Water uptake is ecologically important because it is the universal solvent for all biochemical reactions. Also, water uptake is constantly needed to replace water loss by transpiration. Transpiration is a necessary ecological cost of gas exchange for carbon gain. Rather little is known about the pathway of water movement in roots and the mechanism of water uptake. Even less is known about the comparative ecophysiology of water uptake between species. A few instances are discussed in Section 5.6 of this chapter and rather more can be learned in a recent review of the ecological aspects of root permeability to water (Nardini et al. 2002). Hence, this chapter will concentrate primarily on the mechanism and pathway of water movement in roots.

Water transport across roots is generally described as being purely passive, i.e., it involves no input of metabolic energy. Water is not taken up actively, but instead moves passively through the root in response to a 'force' set up by transpiration. Flow is assumed to be proportional to the force. The force involved is usually equated with the difference in water potential ($\Delta\Psi$) across the root, which is approximately true for high flow rates, but becomes increasingly inaccurate at low flows. This is in contrast to ion uptake by cells, which often involves an active process requiring the input of metabolic energy and the mediation of ion pumps located in membranes.

In this chapter, we will review what is known about the biophysics of water transport across roots, i.e., the equations that describe transport and how the equations relate to root anatomy. Along the way we will review the current methods used to measure root conductance, how solute and water transport are coupled and the experimental approaches used so far to quantify the dis-

tribution of hydraulic resistances along the water transport pathway, i.e., radially from the root surface to the stele and then axially from the stele to the shoot. The chapter will conclude with a discussion on how to scale root conductance measurements to plant size illustrated with some results and ecological interpretations.

5.2 Root Structure and Possible Pathways of Water Movement

The 'typical' structure of monocot and dicot roots is illustrated in Fig. 5.1. The transport properties of roots cannot be interpreted without a clear understanding of their structure. However, root anatomy is highly variable because major differences are seen between species and between roots of the same species grown in different habitats. There are also differences along the length of an individual root. Common examples for such differences are the formation of aerenchyma and the development of endo- and exodermis, usually with Casparian bands, suberin lamellae, and thickened, modified walls. Roots are also altered by the death of the epidermis or even the entire central cortex or by the development of bark and lateral roots. This means that the knowledge gained on one root is not easily generalized to all roots.

The only good example of a study that correlates structure with the physiology of water and solute uptake is the work done on maize roots grown in hydroponic culture (Peterson and Steudle 1993; Peterson et al. 1993; Steudle et al. 1993). Maize roots are characterized by having a living epidermis and central cortex, an immature exodermis, mature proto- and early metaxylem,

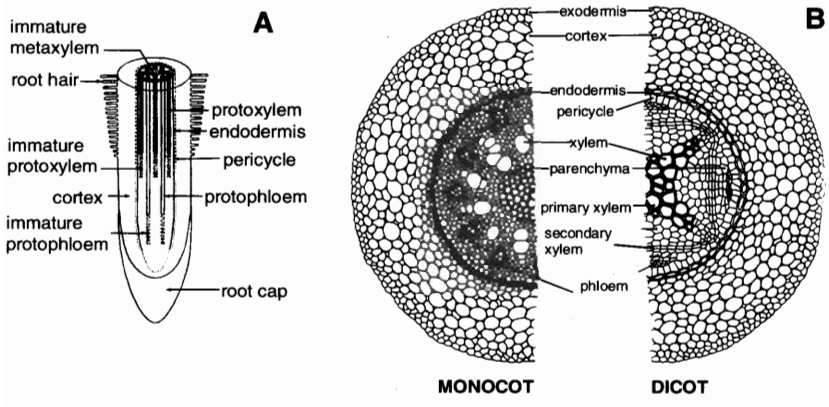

Fig. 5.1A,B. **A** Enlargement of a dicot root tip about 0.6 mm basal diameter. **B** Cross section of monocot and dicot roots. (Adapted from Tyree 1999)

immature late metaxylem (i.e., the vessels still have end walls and living cytoplasm), and an endodermis with Casparian bands, but no suberin lamellae or thickened walls (Fig. 5.2). Towards the tip of the roots there is a hydraulically isolated zone with immature metaxylem and a mature but non-functioning protoxylem.

Many people presume that the Casparian bands or suberin lamellae prevent water moving from epidermis to xylem entirely through cell walls, i.e., forcing water and/or solutes at some point to traverse at least one cell layer by a transcellular pathway en route to the stele. The stele is defined as the morphologic unit of the root consisting of the vascular system and the associated ground tissue – pericycle, interfascicular tissue, and pith (Esau 1960). However, even in the relatively simple and unthickened cortex, it is unclear what the pathway is for water and solute flow. There are three possible pathways: apoplastic, symplastic and transcellular (Fig. 5.3). The part of any plant tissue outside the plasma membrane of the living cells is termed apoplast. It includes cell walls, intercellular spaces, and the lumina of dead cells (e.g., mature vessels and tracheids or dead fiber cells). The symplast is the continuum of cytoplasm interconnected by plasmodesmata and excluding the vacuoles. The terms apoplastic and symplastic transport refer to movements within the two compartments previously defined. While this may be a reasonable definition for ion transport it may not be sufficient for water transport because water permeability across membranes is several orders of magnitude more than for ions. So a third path for water flow (the transcellular path) can be defined as one in which water moves across membranes to get from cell to cell. Two plasma membranes would have to be crossed per cell layer as well as the short distance of wall space between adjacent cells, which is normally presumed not to be rate-limiting. Although we define three pathways, there could be a combination of paths. For example, water flow might be 30 % apoplastic and 70 % transcellular for the whole root radius or the pathways may vary depending on radial position so flow may start out in the symplast for some distance then might pass through a plasma membrane and move within the cell wall for the rest of the path.

Hence, water and solute transport in roots must be viewed as going though a composite membrane consisting of cell walls, membranes and plasmodesmata that are spatially arranged into parallel and serial pathways. Each component (cell wall, membrane and plasmodesmata) will have a different permeability to water and solutes. If we define the whole root annulus from the epidermis to the vessels to be the 'membrane' limiting water and solute transport, then the permeability properties of the root membrane will be a complex function of the sum of these parallel and serial components. A complete discussion of how the transport parameters of a composite membrane relates quantitatively to its components is beyond the scope of this chapter, but such literature can be accessed through Kedem et al. (1962). At this point we do not have enough information about component properties to use existing theory.

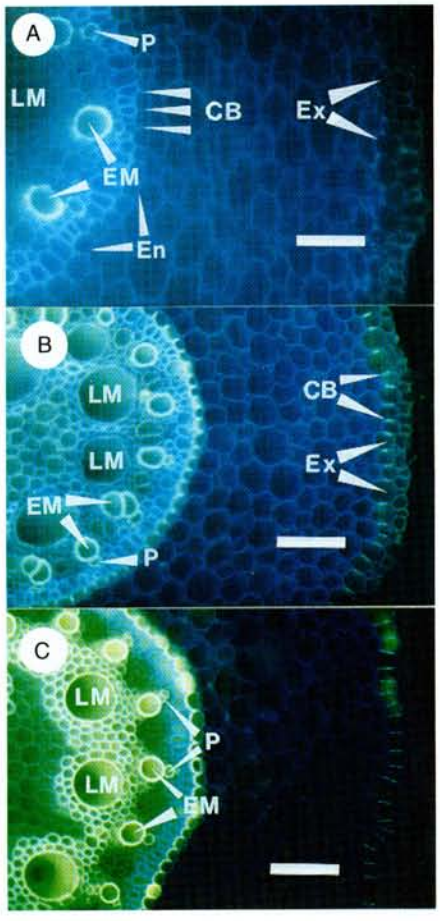

Fig. 5.2A–C. Cross sections of maize primary roots at various stages of development. Specimens were photographed under UV/violet light (wavelength 390–420 nm) following staining with berberine and either aniline blue or toluidine blue O. *Scale bars* 100 μm. **A** Immature exodermis (*Ex*), endodermis (*En*) with Casparian bands (*CB*), mature protoxylem (*P*), mature early metaxylem (*EM*), immature late metaxylem (*LM*). **B** Mature exodermis, endodermis with asymmetrically thickened walls, mature protoxylem and early metaxylem, immature late metaxylem. **C** As in **B**, but late metaxylem (*LM*) is mature. Walls of cells surrounding the late metaxylem are thickened and lignified. (Steudle and Peterson 1998)

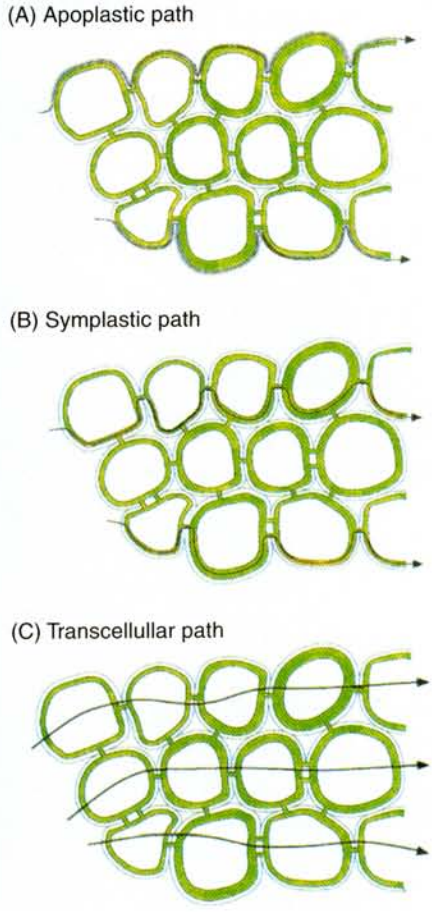

Fig. 5.3A–C. Routes of water flow in plant tissue. The tissue is represented by four cell layers arranged in series. **A** Denotes the apoplastic path (cell walls, *grey*) around protoplasts. **B** The symplastic path is mediated by plasmodesmata, which bridge the cell walls between adjacent cells so that a cytoplasmic continuum is formed (*green*). During the passage of the apoplast and symplast, no membranes have to be crossed. **C** In the transcellular path, two plasma membranes have to be crossed per cell layer. Due to the rapid water exchange between protoplasts and adjacent apoplast, there should be local water flow equilibrium between the two compartments at any time. In the root, the apoplastic flow component is modified by the existence of apoplastic barriers (Casparian bands, suberin lamellae). (Steudle and Peterson 1998)

5.3 Driving Forces and the 'Composite Membrane'

In the classical view, the force acting on water entry into roots is the difference in water potential across the root, $\Delta\Psi$, which is the sum of its osmotic (π) and pressure (P) components:

$$\Delta\Psi=\Delta\pi+\Delta P\cong -RT(C_i-C_o)+(P_i-P_o) \tag{5.1}$$

where RT is the gas constant times absolute temperature, C_i and P_i are the internal solute concentration and pressure, respectively, and C_o and P_o are the external (soil solution) concentration and pressure, respectively, at the surface of the root. Many people seek a functional relationship between the mass or volume of solution passing through roots and $\Delta\Psi$. Since the solution is mostly water having a density near 1 kg/l, mass flow rate in kg/s is nearly the same as l/s. However, the relationship between $\Delta\Psi$ and mass flow (F_m, where most of the mass is water) is more complicated than given by the classical view.

In the classical view, F_m (kg s^{-1} or m^3 s^{-1}) is proportional to $\Delta\Psi$, i.e.,

$$F_m=H_r\Delta\Psi \tag{5.2}$$

where H_r is the root hydraulic conductance (a root water permeability coefficient). The problem with Eq. (5.2) is that H_r was found not to be constant for some roots (e.g., Mees and Weatherley 1957; see Sect. 5.5.) In particular, H_r often appears to change with F_m. Irreversible thermodynamics also tells us that the classical view has to be modified to reflect the fact that $\Delta\pi$ and ΔP have unequal influence on F_m in many situations, e.g., a $\Delta\pi$ of 0.1 MPa might not cause the same flow as a ΔP of 0.1 MPa. One approach to deal with the problem is to introduce another transport constant called the reflection coefficient (σ) which is a number generally between 0 and 1 that measures the relative impact of $\Delta\pi$ versus ΔP on F_m and indicates the impermeability of a membrane to solutes. This permits us to improve the classical equation:

$$F_m=K_r(\sigma\Delta\pi+\Delta P)=K_r[-\sigma RT(C_o-C_i)+(P_o-P_i)] \tag{5.3}$$

where K_r is a different kind of root conductance, which unlike H_r is more likely to be a constant, i.e., independent of the driving forces of $\Delta\pi$ and ΔP. Strictly speaking σ has a different value for each solute interaction with any given 'membrane', but in many experiments only one solute is varied at a time so Eq. (5.3) can be used as a first approximation. Equation (5.3) is more frequently written in terms of flux density, i.e., flow per unit surface area, $J_v=F_m/A_r$, where A_r is the root surface area over which flow is presumed to occur.

$$J_v=L_r(\sigma\Delta\pi+\Delta P)=L_r[-\sigma RT(C_o-C_i)+(P_o-P_i)] \quad (5.4)$$

where $L_r=K_r/A_r$ is a root conductance per unit root-surface area.

The classical equation for solute flux (J_s) in a root can be written as:

$$J_s \cong P_s(C_o-C_i)+J^*_s \quad (5.5a)$$

where J^*_s is the active solute uptake flux density and P_s is the passive permeability of the root to the solute. In many situations Eq. (5.5a) is sufficiently accurate, but in some cases we need to take into account the coupling between flux of water (J_v) and solute so the equation from irreversible thermodynamics is:

$$J_s = \overline{C}_s\,(1-\sigma)J_v + P_s\,(C_o - C_i) + J_s^* \quad (5.5b)$$

and $\overline{C}_s$ is the average concentration of the solute in the root 'membrane'. The first term in Eq. (5.5b) accounts for the influence of water flux density (J_v) on solute flux, the second term accounts for passive diffusion, and the last for active transport.

However, mass flow (F_m) can also be viewed as 'quasi-active' because water flow is coupled to solute flow in Eq. (5.3). This follows because the rate of active solute uptake into a root can change the value of C_i. The coupling between water and solute flux is most when ΔP is small, i.e., usually at times of low transpiration. The situation is even more complex when we view the anatomical details of the pathway of water and solute movement in roots. The different anatomical components of roots provide different pathways for solute and water flow with each pathway having potentially different transport permeabilities. Hence, Steudle has argued that we must view roots as composite membranes (Steudle et al. 1993; Steudle and Frensch 1996; Steudle and Peterson 1998).

Some information can be gained about the role of cell types in the transport of water and solutes in roots by measuring transport of water and solutes in roots before and after damaging different cells or regions of roots. However, before entering into a detailed discussion of what has been learned about maize roots, we need to digress to discuss methods used for measuring water and/or solute transport in root systems.

5.4 Methods of Measuring Hydraulic Conductances

A number of different methods have been used in the past for measuring solute and water transport in excised root systems. In most instances, roots were measured while immersed in aqueous solution so that the experimenter

had better control of the solute composition and concentration. Roots were grown either in hydroponic culture or in soils and extracted to the aqueous solutions in the measuring apparatus.

5.4.1 Root Chamber Methods

Fiscus (1977) was one of the major users of the root chamber method for measuring hydraulic properties of roots. This method is generally used for measuring steady-state fluxes of water and solute on large root systems. A root system is enclosed in a metal chamber. The root medium is generally an aqueous solution of known composition, but it can also be a soil. The pressure of the root medium can be adjusted by connecting the root chamber to a compressed air source (Fig. 5.4A). The root system is excised together with a length of stem, which passes out of the root chamber via a rubber seal. The stem is connected to water-filled pipes and valves, which in turn are connected to pressure sensors or flow sensors. Many roots will exude solution and the rate of exudation can be measured by opening the valve to the flow sensor. Exudation occurs because the root accumulates solutes increasing C_i above C_o in Eq. (5.3) causing a flow even when $P_i=P_o$. By measuring the flow rate of exudation (F_m) and the concentration of a given solute in the exudates (C_{si}, mol kg^{-1}) the rate of solute uptake (F_s, mol s^{-1}) can be estimated under steady-state conditions from $F_s=F_mC_{si}$. F_m is usually measured by directing flow to a balance and measuring the weight of root exudates at fixed time intervals. The root pressure under zero flow can also be measured by closing the valve to the flow sensor. Flow rate can also be measured as a function of (P_o–P_i) because the value of P_o can be changed by admitting gas into the chamber from the compressed air source (Fig. 5.5A).

5.4.2 Nobel Method

The Nobel method is a very simple technique that has been used on small root systems extracted from soil; the method is used to estimate steady-state solution flow through roots resulting from an imposed pressure drop (P_o–P_i). A root is sealed to a capillary tube and immersed in solution. A partial vacuum of 10–50 kPa is drawn from the end of the capillary tube, which induces water uptake. Solution flow through the root is computed by noting the rate of advance of the air/water interface in the capillary tube. A plot of flow versus pressure drop is similar to that in Fig. 5.5A. The same method can be used to estimate the vascular resistance to water flow by mounting a root segment in the capillary tube rather than a whole root. A possible disadvantage of the Nobel method is that flow rates and applied pressure drop are smaller than

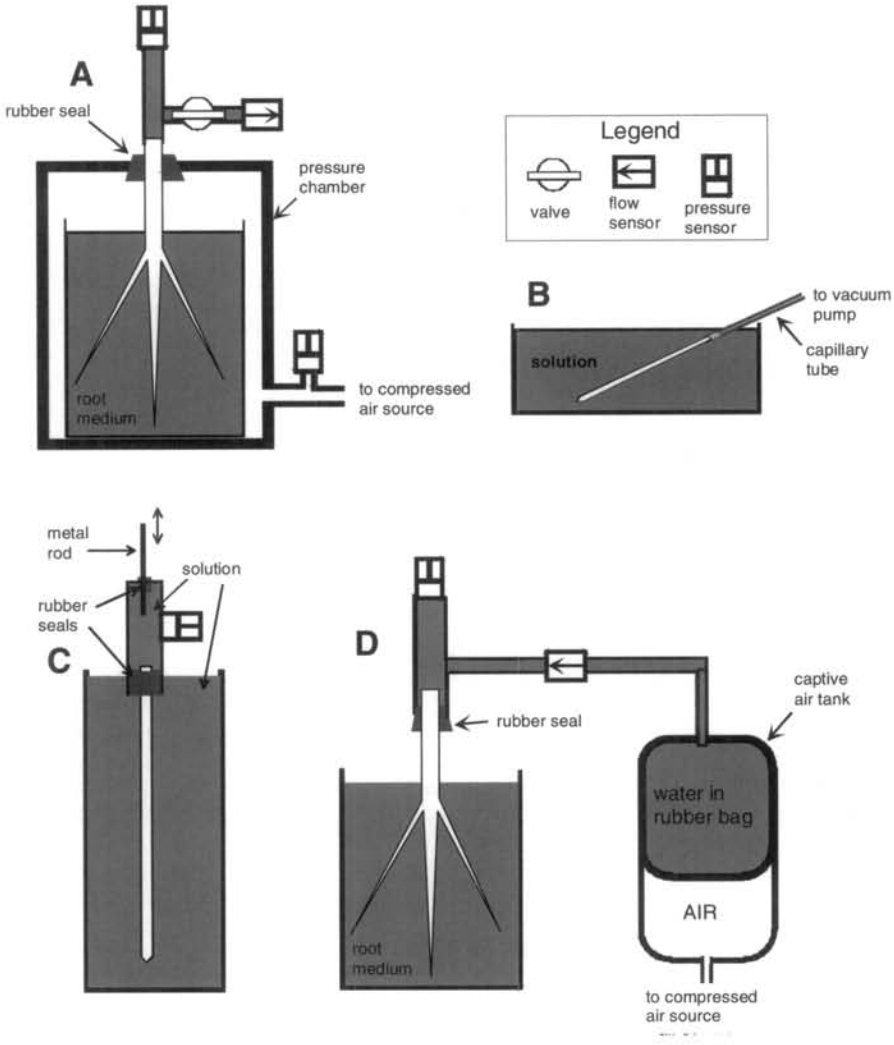

Fig. 5.4A–D. Methods for measuring root transport properties. **A** Root chamber method. **B** Nobel method. **C** Root pressure probe (RPP) method. **D** High-pressure flowmeter (HPFM) method. See text for details

normal physiological ranges, hence the data could be influenced by osmotic contributions to flow in plants with high rates of active uptake of solutes (see Eq. 5.4).

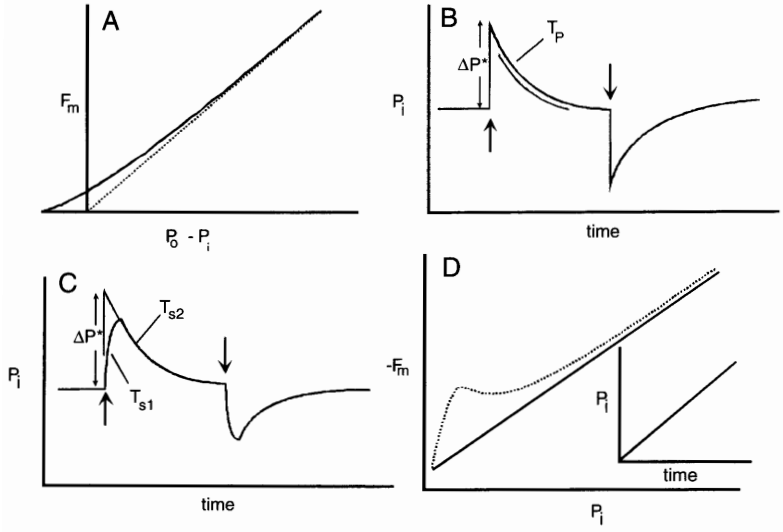

Fig. 5.5A–D. Examples of experimental results from the methods in Fig. 5.4. **A** Typical relationship between mass flow (F_m) and pressure difference across root (P_o–P_i) obtained for steady-state experiments by the root chamber and Nobel methods. *Dashed line* Results when there is no osmotic pressure difference across the root; *solid line* results when there is active solute uptake and hence osmotic pressure differences are a function of flow and uptake rate. **B** and **C** Typical results for the root pressure probe. See text for details. **D** Typical experimental results with the high-pressure flowmeter (HPFM). *Inset* Flow P_i versus time imposed by the HPFM and the main graph gives the resulting flow versus P_i. *Solid line* shows the result with no air present in the root system and the *dotted line* is a typical result when some air is present. See text for details

5.4.3 Root Pressure Probe Method

Steudle (1993) developed the root pressure probe (RPP), which is a variation on a cell pressure probe (Fig. 5.4C). The RPP uses a pressure relaxation method (dynamic method) for measuring solute and water transport parameters of root systems. The RPP has the advantage over all other methods because it can be used to measure all the important parameters for solute and water transport, i.e., L_r, σ, and P_s (see Eqs. 5.4 and 5.5). The RPP works best with small root systems but has also been used with larger, branched root systems of relatively small seedlings. A root is excised and the basal end is sealed into a plastic chamber filled with solution. The pressure of the fluid is measured with a pressure sensor and the pressure can be dynamically altered either by moving a metal rod, also sealed into the chamber, or by changing the solution concentration in the external solution (C_o).

The root reaches a stable internal pressure (P_i) after it has been mounted in the pressure probe for several hours. A typical pressure relaxation experiment

is illustrated in Fig. 5.5B. At the up-arrow the metal rod is rapidly advanced into the RPP displacing a known volume of solution, ΔV, which causes an initial pressure increase, ΔP^*. The ratio $\Delta P^*/\Delta V$ is a measure of the absolute elasticity of the root plus pressure probe. The increase in pressure immediately causes an efflux of water and a gradual relaxation of the pressure. By analysis of the relaxation curve, the value of L_r can be determined provided the absolute elasticity is a constant, i.e., provided ΔP^* is a linear function of ΔV during the pressure relaxation. If air bubbles are present in the root (either in vessels or intercellular spaces) this requirement of constant elasticity is not met because some of the volume displacement of the rod goes to compress the bubbles and pressure of the bubbles is inversely proportional to the volume (based on the ideal gas law). Hence the root system has to remain under pressure for many hours to dissolve all the air bubbles prior to measurement. If the metal rod is withdrawn rapidly from the RPP (down-arrow, Fig. 5.5B), the pressure change and relaxation is in the opposite direction.

The relaxation curve has a half-time, T_p, which describes the rate at which ΔP approaches zero, and the root conductance, L_r, is calculated from:

$$L_r = \frac{\Delta V}{\Delta P^*} \frac{T_P}{A_r \ln(2)} \tag{5.6}$$

where A_r is the root surface area. Equation (5.6) is valid only for an exponential decay process. Generally the shape of the relaxation curve is not a true exponential decay of ΔP, but the middle portion of the curve (highlighted by dots in Fig. 5.5B) is approximately exponential. The computation of L_r of Eq. (5.6) has been validated by independent measurements of L_r.

The pressure changes in Fig. 5.5C can also be induced by rapid changes in C_{so} of a solute in the solution bathing the root. If C_{so} is changed from an initially high to low value (up-arrow, Fig. 5.5C) the pressure increases. The time delay for the increase in pressure, T_{s1}, is presumed (by the author, see Sect. 5.5) to be due to the time for the solute to diffuse through unstirred layers and root tissue to reach the solute permeability 'membrane', which is presumed to be the endodermis. The second time delay (half-time, T_{s2}) is governed by the time it takes the solute to permeate from outside the root to the xylem conduits. The permeability of the root to the solute is computed from:

$$P_{sr} = \frac{V_x}{A_r} \frac{T_{s2}}{\ln(2)} \tag{5.7}$$

where V_x is the volume of the xylem conduits.

The reflection coefficient can be calculated from the initial change in pressure and concentration, $\sigma = \Delta P^*/RT\Delta C_{so}$; when $T_{s1} << T_{s2}$ the value of ΔP^* is easily evaluated, but when T_{s1} and T_{s2} are more nearly equal then a small correction has to be made for the probable ΔP^* by extrapolating the T_{s2} curve

back to 'time zero' when the solution concentration was changed (as shown in Fig. 5.5C).

When C_{so} is increased from a low to a high value the initial pressure change and relaxation will be in the opposite direction (down-arrow, Fig. 5.5C).

5.4.4 The High-Pressure Flowmeter Method

The high-pressure flowmeter (HPFM) method was developed by Tyree et al. (1995) to provide dynamic and steady-state measurements of root and shoot hydraulic conductance. In roots it is best to use the dynamic method (Tyree et al. 1994). The HPFM method can be used on much larger root systems than the RPP method. There is some overlap in measurable root sizes by both methods, i.e., the smaller root sizes measurable by the HPFM overlap with the larger root sizes measurable by the RPP. The HPFM method has been calibrated versus the pressure chamber method and both methods produce comparable values of K_r (Eq. 5.3).

In the HPFM method a root system in solution or soil is excised from the shoot and connected to the HPFM via a rubber seal (Fig. 5.4D). The pressure (P_i) is measured above the excised root as well as the flow into the root. The value of P_i is controlled by adjusting the air pressure in a captive air tank (CAT) where water is held in a rubber bag inside the CAT. As P_i increases water flows into the base of the root and exits through the root surfaces, so flow is opposite to the direction during transpiration. In a typical dynamic measurement, air is admitted into the CAT at a constant rate causing a linear increase in P_i versus time (Fig. 5.5D, insert). Typically, the pressure is increased from 0 to 0.5 MPa. If no air is present in the root, a plot of F_m vs. P_i is linear (Fig. 5.5D, solid line) with a non-zero y-intercept caused by the elasticity of the root plus HPFM. The slope of the line equals K_r.

Generally, there is some air present in the root being measured, but the accuracy of K_r determined by the HPFM is not as seriously affected by air as in the RPP method so a long period of pre-pressurization is not required. When a moderate amount of air is present a curve like the dashed line (Fig. 5.5D) is found, but the limiting slope at high P_i is the same as for a root without air. However the HPFM does overestimate K_r in large woody root systems when a lot of air is evenly distributed throughout the wood.

The advantage of the HPFM over the RPP is that many roots can be measured per day; the time required to mount and measure a root is typically 10–20 min per root. Also the HPFM can be used on plants growing in soil in pots or growing in the field.

5.5 Distribution of Hydraulic Resistances in Roots

Generally, the axial resistance to water flow in roots is much less than the radial resistance. This is because axial flow is carried by vessels or tracheids whereas radial flow involves passage of water through non-vascular tissue. It is often assumed that the main barriers for radial flow of solutes and water are both in the endodermis, but some experiments have shown otherwise.

5.5.1 Axial Water Flow – Poiseuille's Law

Axial hydraulic conductivity in roots tends to increase from apex to base, i.e., with root age, because as roots get older the number and/or diameter of vascular conduits (vessels or tracheids) tend to increase. Poiseuille's law states that the hydraulic conductance of a cylindrical pipe of uniform diameter increases with the fourth power of the diameter. Poiseuille's law does not strictly apply to vascular conduits in roots, because they are not cylindrical nor of uniform diameter along their lengths, but Poiseuille's law does provide a useful first approximation, so for a root segment with n vessels of diameter d:

$$K_{axial} = \sum_{i=1}^{n} \frac{\pi \ d_i^4}{128\eta L} \tag{5.8}$$

where η is the viscosity of the solution in the vessels and L is the length. Steudle and Peterson (1998) report that young maize roots have protoxylem vessels near the tip that are 5–10 μm in diameter, then 25 mm from the tip early metaxylem vessels are 23 μm, and, finally, at distances of 250 mm from the tip, the late metaxylem elements are about 100 μm. So Poiseuille's law would predict that one old metaxylem vessel would be as conductive as 357 early metaxylem vessels. There are typically 14 early metaxylem vessels versus 7 late metaxylem vessels. If we compare the hydraulic conductance of 100 mm of root with early metaxylem versus 100 mm of root with late metaxylem, the old metaxylem part of the root would have an axial conductance that is 179 times that of the early metaxylem part. The theoretical axial conductance of maize roots is much more than the total root conductance and this has been confirmed experimentally as indicated below. Hence the radial (non-vascular) path limits the rate of water flow through roots.

5.5.2 Radial Water Flow and Role of Endodermis and Exodermis

Root conductivities per unit surface area, L_r, have been measured on maize roots about 1 mm diameter and 200–500 mm long by the RPP method and values tend to be around 2.3×10^{-5} kg s^{-1} m^{-2} MPa^{-1} (Steudle and Peterson 1998). These values agree with those measured by more traditional methods (Newman 1973; Miller 1985). The 225 mm length of maize root containing early metaxylem has a surface area of $A=7 \times 10^{-4}$ m^2, hence K_r for that region is $AL_r=1.6 \times 10^{-7}$ kg s^{-1} MPa^{-1} or a resistance of 6.2×10^6 MPa s^{-1} kg^{-1} ($=1/1.6 \times 10^{-7}$). The 14 early metaxylem vessels in this same length of root would have an axial conductance of 4.4×10^{-7} (from Eq. 5.6) or a resistance of 2.25×10^6. Hence, in young roots, the radial resistance is two to three times the axial. In slightly older maize roots with old metaxylem we have already shown that the axial resistance of the same 225 mm would be 179 times less, hence the radial resistance would be 300–500 times more than the axial resistance. Clearly, the ratio of resistance depends rather strongly on the diameter and number of xylem conduits in the roots so the theoretical calculations are rather approximate. However, these theoretical calculations are consistent with experiments on young roots in which hydraulic resistance is measured before and after root tips are excised, which decreases the resistance by a factor of 3–20.

5.5.3 Experiments to Locate Major Barriers to Water and Solute Flow

From the above considerations we can conclude that the main barrier to water flow may be non-vascular, i.e., somewhere in the radial pathway. But where in the radial pathway is the barrier located and is it at the same location for water and solutes? Some useful insights result from wounding experiments in which the effect of mechanical damage to the cortex and/or endodermis is measured in terms of the effect of such damage of root pressure, reflection coefficient, hydraulic conductivity and solute permeability.

The Casparian band is thought to reduce the water permeability of the cell walls in the endodermis forcing the pathway of water movement to be transcellular in the vicinity of the endodermis. Hence water would have to pass through at least two plasmalemma membranes. The surface area of this membrane pathway would be at least as great as the surface area of the endodermis. The area could be more if a significant fraction of the water transport is symplastic via plasmodesmata, hence water could enter through several layers of cortical cells, pass through the symplast, then exit through several layers of cells in the stele before reaching the xylem conduits. This notion is approximately consistent with observed values of root and membrane conductance. Maize root conductance (Steudle et al. 1993) measured on roots 90–180 mm long and 1 mm diameter is about 2.7×10^{-8} m s^{-1} MPa^{-1} (normalized to the epidermal surface area) and, since the endodermis is about half the

diameter of the epidermis, the conductance normalized to the endodermis surface would be about double (5.4×10^{-8}). In contrast, maize-root, cortical-cell membrane conductance is 2.4×10^{-8} m s^{-1} MPa^{-1} (as measured by a cell pressure probe) so the conductance of two membranes in series would be 1.2 $\times 10^{-8}$ or about one-quarter that of the root conductance normalized to the endodermal area. From this we can conclude that the membrane (transcellular) pathway accounts for at least one-quarter of the root conductance and the rest is via the apoplast. Alternatively, a larger fraction of the root conductance could be transcellular if water enters several cells, and thus through a much larger area of membrane, and then travels through the symplast. In an earlier study where 90 measurements were done on shorter maize roots (70–110 mm), L_r=1.1±0.1 $\times 10^{-8}$ (mean and SEM, Steudle et al. 1987) and cortical-cell membrane conductance was again 2.4±0.3 $\times 10^{-8}$, so from these data we might conclude that about half the hydraulic resistance to water transport was transcellular across two membranes in the endodermis.

Wounding experiments provide more insights. Maize roots (90–180 mm long and 1 mm diameter) were mounted in a RPP until a stable root pressure (P_i) of 0.15±0.03 MPa was reached (Peterson et al. 1993; Steudle et al. 1993). A fine glass rod was inserted radially 400 μm into the roots causing a 20 μm diameter wound in the endodermis ($<10^{-4}$ or 10^{-5} of the endodermal surface area). The wound caused a rapid (100–200 s) drop in root pressure to 0.05±0.01 MPa, but no significant change in L_r. When P_i is constant in a RPP there is no water flow [F_m=0 in Eq. (5.3)]. Setting F_m=0 in Eq. (5.3) and solving for P_i (the root pressure) it follows that:

$$P_i=P_o-\sigma RT(C_o-C_i) \tag{5.9}$$

Since P_o=0 (atmospheric pressure) and C_o is unchanged, the rapid drop in root pressure could only be due to a rapid drop in C_i along the whole length of the xylem vessels. Diffusion would be too slow to account for the drop of C_i in <200 s, hence there must have been a mass flow leak of xylem sap through the wound. From this Steudle et al. (1993) conclude that the endodermis is the principle barrier to solute diffusion but not to water flow (otherwise L_r would also have increased). I am not convinced by the argument regarding water flow, because a wound to $<10^{-4}$ of the endodermis root surface would be effective only if all the water could freely exit through a very small surface area of cells in the stele and this resistance is unknown but probably high. In other experiments, Peterson et al. (1993) removed rather larger fractions of the cortical tissue of maize roots (15–38 %) and this caused an approximately proportional increase in L_r, from which they conclude (rather more convincingly) that the barrier to water flow is diffusely distributed over the entire cortex.

Another approach to the location of the water barrier is to measure the pressure drop across the radius of a root while water is flowing; the principle hydraulic resistance would correspond to the region with the biggest drop in

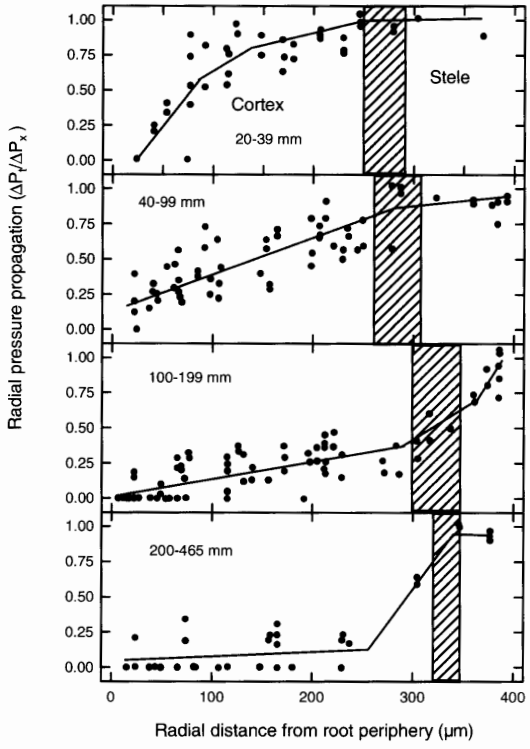

Fig. 5.6. Radial propagation of pressure across the cortex in four different zones of a maize root. Data points represent turgor responses (ΔP_t) following either an increase or a decrease in xylem pressure (ΔP_x). Locations of the endodermis within each zone are marked by *cross-hatched areas*, as determined by microscopic observations. Pressure gradient trend lines are drawn in *by hand*; steeper slopes indicate where the hydraulic resistance is most. (Adapted from French et al. 1996)

pressure. This has been accomplished more or less directly in experiments done on 500 mm long maize roots by Frensch et al. (1996). They used a cell pressure probe to measure changes in cortical and endodermal cell turgor pressure resulting from changes in xylem pressure. Although we do not know if the main pathway is transcellular or apoplastic, the changes in cell turgor should reflect changes in apoplastic pressure in adjacent cell walls. Results were obtained for root regions of different ages, i.e., different distances from the root tip (Fig. 5.6). Over the first 100 mm of the root (measured from the tip) there is a more or less uniform pressure gradient from the stele to the epidermis, which is consistent with the earlier finding. In the next section (100–200 mm from the tip) about two-thirds of the pressure drop is across the stele and endodermis and the rest across the cortex. For the oldest portions of the root (>300 mm from the tip) almost all the pressure drop is across the endodermis and adjacent cortical cells. Hence the situation is more complex than one might conclude from experiments on young roots 90–180 mm long.

5.6 Models of Solute and Water Flux in Roots (Possible Reinterpretation of Ideas)

Space does not permit a full quantitative description of existing models of transport of water and solutes in roots, but a brief examination is useful. The differences between models involve: (1) the use of classical transport equations versus irreversible thermodynamics transport equations (Eqs. 5.2 and 5.5a vs. Eqs. 5.4 and 5.5b), (2) treating the root 'membrane' as a simple barrier versus a composite 'membrane', and (3) treating the xylem sap inside the root vessels as a single compartment or treating the root as multiple cylindrical compartments in a linear catena.

Early experimenters assumed that classical equations provided an adequate quantitative model and for many root systems this was true. However, sometimes plots of mass flux (F_m) versus ΔP were non-linear (as in Fig. 5.5A), i.e., the root conductance H_r increased with increasing flow (Lopushinsky 1964). In extreme cases plots of F_m versus $\Delta\Psi$ showed negative H_r, i.e., flow opposite to the direction of the driving force for small flows (Mees and Weatherley 1957).

In any quantitative model, it is best (most ideal) to have transport coefficients, e.g., L_r, P_s and σ, that are independent of the driving forces. The transport equations from irreversible thermodynamics promise to fulfill this ideal. Fiscus (1975) was the first to demonstrate that the application of transport equations from irreversible thermodynamics in a root model with a simple membrane and only one compartment could explain the anomalous changes in H_r. Unfortunately, Fiscus (1975) still talked about the 'apparent resistance' ($=1/H_r$) being a function of flow; this still leads to confusion today because in reality the transport coefficients for a root are constant, i.e., L_r (as well as P_s and σ) do not need to change with flow to account for a non-linear relation in plots of J_v vs. $\Delta\Psi$ or ΔP as shown by the model of Fiscus (1975).

The elucidation of the composite membrane model (e.g., Steudle 1994) has provided further insights into the complexity of solute and water flow along the root radius. The mathematical descriptions advanced by Steudle (1994) emphasize the parallel composite properties of the root–membrane complex and a single xylem sap compartment. Steudle and Peterson (1998) suggest that the parallel composite membrane model explains: (1) why root hydraulic conductivity appears to change with flow rate, (2) why there are differences between hydraulic conductivity when measured with hydrostatic pressure or osmotic pressure gradients, and (3) why roots have a low reflection coefficient, σ. In reality, however, the root–membrane is a very complex system of parallel and serial membrane components and it is unclear if a parallel model will ultimately prove to be adequate. Hence the conclusions drawn (e.g., Steudle 1994; Steudle and Peterson 1998) may be subject to alternative interpretations and will be discussed briefly below.

Root hydraulic conductivity may not increase with flow. Plots of F_m vs. $\Delta\Psi$ are frequently curvilinear and the slope of this curve, H_r, does change with F_m. However, this does not mean that root hydraulic conductivity, L_r, is changing. So the composite membrane model really does not predict changes in L_r. There are theoretical cases in which root hydraulic conductivity may change with flow *if L_r is controlled by root membrane permeability to water*. In this case the genetic expression of root aquaporins may cause a change in membrane permeability to water and hence L_r of roots (Steudle and Henzler 1995). Recently, Tsuda and Tyree (2000) have attributed the diurnal variation in L_r of sunflower roots to diurnal variation in expression of aquaporins. Recently Siefritz et al. (2002) has demonstrated that aquaporins account for about half the root conductance in tobacco.

In some root systems the value of root hydraulic conductivity is less when measured by flow induced by osmotic pressure changes (L_{ro}) versus hydrostatic pressure changes (L_{rp}). In maize roots L_{ro} is 10 times less than L_{rp} and in *Quercus robur* roots L_{ro} is 100 times less than L_{rp} (Steudle and Peterson 1998). With reference to the parallel composite membrane model, this difference between L_{ro} and L_{rp} could be explained if osmotic flow is via a transcellular pathway and pressure flow is via an apoplastic pathway and this is a plausible explanation, theoretically. An alternative possibility is that the RPP is not measuring L_{ro} correctly.

In the RPP method, L_{ro} is computed from the half-time of the initial change in pressure (P_i) following the change in external osmotic pressure, RTC_o (see T_{s1} in Fig. 5.5C). Two processes must occur immediately after a change in C_o; for example, if C_o is increased, then the solute must first diffuse to the selective (semipermeable) membrane and then water must flow out of the root to lower P_i. The time constant, T_{s1}, could be a measure of the time for the solute to diffuse to the membrane or could be a measure of the time for water to pass out of the root via the membrane, or a combination of the two. In comparable experiments using a cell pressure probe on single cells, the water permeation through the cell membrane is the limiting process. In roots, however, this may not be the case if the selective membrane is located at the endodermis (either the plasmalemma membranes of the endodermal cells or the Casparian band). Let us say that the solutes reach the endodermis by diffusion through the apoplast of the epidermis and cortex, i.e., the cell walls. The direct radial distance is 250–350 μm in maize but the actual tortuous path length is more likely to be 400–500 μm (Fig. 5.3A). The solutes have to diffuse this distance through water; the diffusion coefficients, D, for the solutes used in RPP experiments range from 1.8×10^{-9} to 1.5×10^{-9} m^2 s^{-1} for KNO_3 and NaCl, respectively, to 0.68×10^{-9} to 0.52×10^{-9} for manitol and sucrose, respectively, in pure water. In the confines of the cell walls, the values may be somewhat lower, so let us use a range of 1.5×10^{-9} to 0.4×10^{-9} m^2 s^{-1}. The time, t, it takes half the molecules to diffuse a distance x is given by $t=x^2/2D$. Using all possible values of x and D above we have a predicted range of 53–313 s for the diffusion time

compared with T_{s1} values of 34–690 s (Steudle et al. 1987). The diffusion times may be somewhat longer because of solute/water drag problems. Some molecules will reach the endodermis in less time than above which will initiate outwardly directed osmotic flow of water. The water flow will tend to sweep the solutes away delaying their arrival.

The reflection coefficient, σ, of the common solutes used in RPP measurements of maize range from 0.4–0.85 (Steudle and Peterson 1998). In contrast, these same solutes have reflection coefficients (σ_m) from 0.9–1.0 when measured on plasmalemma membranes of plant cells. In the parallel composite membrane model one of the parallel paths involves plasmalemma membranes and the other the Casparian band, which is presumed to have a low reflection coefficient (σ_c). According to the parallel composite membrane model, σ of the whole root would be a weighted average of the fractional cross-sectional areas and hydraulic conductivities of the two parallel paths. The point of time at which σ is evaluated is generally after 2 to 4 half-times (T_{s1}) and when solute flow approaches zero, so solute/water drag effects are also reduced. So the values of σ are probably much less prone to errors than is the evaluation of L_{ro}. However, this has never been verified by theoretical computations of the dynamics of diffusion and solute/water drag coupling inside the cortical cell walls.

In other types of experiments (Zhu et al. 1995; Schneider et al. 1997) σ has been evaluated in roots attached to transpiring plants. In this situation solute/water drag can cause substantial errors in the estimation of σ. This is because the constant inflow of water to the endodermis can raise the concentration of the solute at the endodermis (C_{oe}) to a value much more than C_o. Measurements of P_i were made with a cell pressure probe positioned in a xylem vessel of a root during steady-state transpiration and looking at the effect on P_i of increasing external solute concentration from zero to C_o. The reflection coefficient was calculated from:

$$\sigma = \frac{\Delta P_i}{\Delta \pi_o} \cong \frac{\Delta P_i}{RT\Delta C_o} \tag{5.10}$$

During this experiment, the flux of solution through the cortical apoplast to the endodermis, J^*_v, is transporting solute at a rate given by CJ^*_v at any given point where the solute concentration C is causing an accumulation of solute concentration towards the endodermis. At any given point the solute is diffusing out at a rate given by Fick's law and at steady state the solute/water drag and diffusion would balance:

$$CJ_v^* = D\frac{dC}{dx} \tag{5.11}$$

The solute/water drag will be most if all the water flux into the root passes through the cortical cell walls; in this case:

$$CJ_v^* = D\frac{dC}{dx} \tag{5.12}$$

where α is the fraction of the root surface area occupied by water in the apoplast. The wall area is about 2 % of the surface area and about half the wall is solid so $\alpha \approx 0.01$.

An approximate solution of Eq. (5.11) results by treating the cortical layer as a plane rather than a cylindrical annulus. Integration of Eq. (5.11) from $x=0$, $C=C_o$ to the endodermis where $x=\delta$ and $C=C_{oe}$ and substitution of Eq. (5.12) for J^*_v yields:

$$\frac{C_{oe}}{C_o} = \exp\left(-\frac{L_r(\sigma\Delta\pi - P_i)\delta}{\alpha D}\right) \tag{5.13}$$

Under a range of transpirational conditions (darkness and humid air to high light and dry air) the value of P_i ranged from +0.08 to –0.2 MPa in maize plants. After adding 50 mol/m^3 NaCl and observing the change in P_i, the value of σ, computed from Eq. (5.10), ranged from 0.15 to 0.9 (Schneider et al. 1997). However, Eq. (5.10) does not take into account the solute/water drag effects in Eq. (5.13). Not enough information is provided in the original publications to estimate J^*_v from Eq. (5.13), but the maize plants went from guttation flow (in darkness and humid air) to high transpiration rates (because of high light and dry air), so $(\sigma\Delta\pi - P_i)$ probably changed by 0.25 MPa, e.g., from –0.04 to –0.29 MPa, before the application of NaCl. Since transpiration rate is limited by vapor-phase resistances (through stomata), we can assume J^*_v did not change after application of NaCl. Assuming $L_r=2.4 \times 10^{-7}$ m s^{-1} MPa^{-1}, $\delta=4 \times 10^{-4}$ m, $D=1.2 \times 10^{-9}$ m^2 s^{-1} for NaCl in cell walls, and $\alpha=0.01$, Eq. (5.13) predicts $C_{oe}/C_o=1.38$ and 10.17 for $(\sigma\Delta\pi - P_i)=-0.04$ and –0.29 MPa, respectively. Space does not permit a more rigorous derivation for cylindrical geometry, but for this case $C_{oe}/C_o=1.43$ and 13.64 with the parameters above. Hence the six-fold change in σ from 0.15 to 0.9 could be accounted for by the difference between C_{oe} and C_o brought about by the solute/water drag effect even if part of the water entering the root is via the transcellular pathway, which would make J^*_v correspondingly smaller. From the above argument it would appear that σ may not be a function of water flow rate in roots.

Tyree et al. (1994) have advanced a root model, AMAIZED, consisting of n root segments with each segment being a link in a catena transport model with a simple root membrane. The AMAIZED model has been used to examine solute and water transport both for the steady state and dynamic situations where solute fluxes and water fluxes are constantly changing with time

and position along the root. The model has been applied to large root systems consisting of an absorbing zone, i.e., young roots where there are radial and axial fluxes of water and solute, and in transport zones, i.e., older (perhaps woody) roots where only axial fluxes occur. A surprising prediction of AMAIZED is that roots with short absorbing zones have the same dynamics as roots with long absorbing zones if all other parameters are the same; this makes modeling of large root systems more feasible and meaningful theoretically. Tyree et al. (1994) excised large walnut root systems and attached an early version of an HPFM to the base. They measured flow versus applied pressure for stepwise changes in pressure (150 to 180 s steps). The model has been very good at predicting the dynamics of pressure-driven water flow (Fig. 5.7).

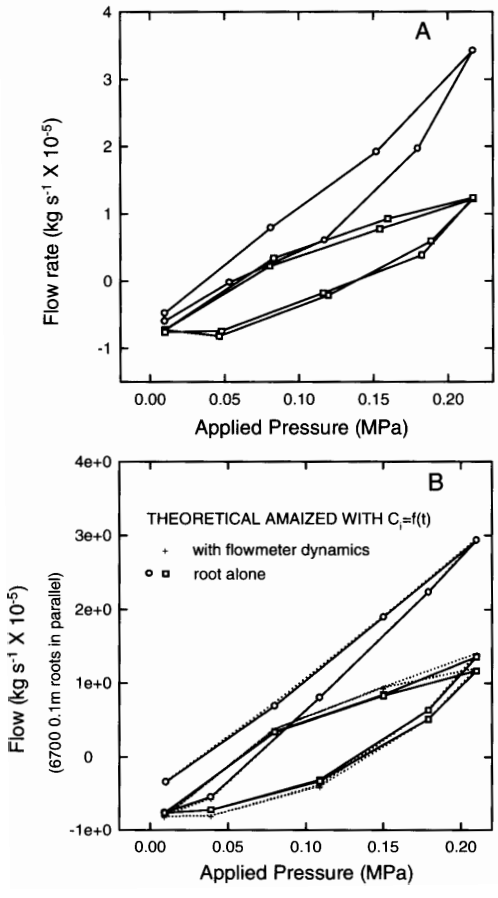

Fig. 5.7A,B. **A** Dynamic measurement of flow versus applied pressure in walnut (*Juglans regia* L. cv. Lara) roots growing in 200-l pots using a high-pressure flowmeter (HPFM). Pressure was adjusted over 150 to 180 s and flow readings were taken at the end of each period. The *arrows* indicate the direction of pressure change. *Open circles* are values measured 20 min after excising the shoots; *squares* are values measured 2 h after excising the shoot. **B** Theoretical predictions from AMAIZED, the model for dynamics of solute and water transport in roots. *Solid lines with open circles* are predictions of AMAIZED 20 min after excising the shoots; *solid lines with squares* are predictions of AMAIZED 1.5 h after excising the shoot; +'s, predictions of AMAIZED with the response time of both the root and HPFM are taken into account. Because +'s are close to open and filled circles, we can conclude that the hysteresis was due to the dynamics of the root rather than the response time of the HPFM. (Adapted from Tyree et al. 1994)

5.7 The Problem of Scaling for Root or Plant Size

The invention of the HPFM has permitted the rapid measurement of root conductance, K_r (kg s^{-1} MPa^{-1}), in both laboratory and field situations on a wide range of root systems sizes, e.g., root systems with basal diameters of 1–25 mm. The value of K_r increases with root or plant size. Root or plant size can be measured in terms of root surface area, A_r, root length, L, total root dry weight, *TRDW*, or leaf surface area, A_L. So this raises the question on how best to scale for size and what can be learned from different ways of scaling.

Since we have already established that radial root resistance is generally more than axial resistance, water uptake is likely to be limited by root surface area. Hence it is reasonable to divide K_r by A_r yielding L_r, which is a measure of root efficiency. Some roots are more efficient than others. Division of K_r by total root length (L) is not as desirable, but is justified because A_r and L are correlated approximately and L can be estimated by a low-cost, line-intersection technique rather than a high-cost, image-analysis technique.

Scaling by root mass is justified by consideration of the cost of resource allocation. Plants must invest a lot of carbon into roots to grow and to maintain them. The benefit derived from this carbon investment is enhanced scavenging for water and mineral nutrient resources. Total root dry weight (*TRDW*) is a measure of carbon investment into roots. Thus the carbon efficiency of roots might be measured in terms of $K_r/TRDW$, $A_r/TRDW$, or $L/TRDW$. Scaling by *TRDW* provides information of ecological rather than physiological importance.

Scaling of K_r by leaf surface area (A_L) provides an estimate of the 'sufficiency' of the roots to provide water to leaves. The physiological justification of scaling K_r to the leaf surface area (A_L) comes from an analysis of the Ohm's law analogue for water flow from soil to leaf (van den Honert 1948). The Ohm's law analogue describes water flow rate (F_m, kg s^{-1}) in terms of the difference in water potential between the soil (Ψ_{soil}) and the leaf (Ψ_L):

$$\Psi_{soil}-\Psi_L=(1/K_{soil}+1/K_r+1/K_{sh})F_m \tag{5.14}$$

where K_{soil} is the hydraulic conductance of the soil. It is usually assumed that $K_{soil} >> K_r$ and K_{sh} except in dry soils so $1/K_{soil}$ can be ignored. Leaf water potential is then approximated by:

$$\Psi_L \cong \Psi_{soil}-(1/K_r+1/K_{sh})F_m \tag{5.15}$$

Or, if we wish to express Eq. (5.15) in terms of leaf area and average evaporative flux density (E), we have:

$$\Psi_L \cong \Psi_{soil}-(1/K_r+1/K_{sh})A_L E \tag{5.16}$$

This equation also can be rewritten so that root and shoot conductances are scaled to leaf surface areas, i.e., to give leaf-specific shoot and root conductances, K_{sh}/A_L and K_r/A_L, respectively:

$$\Psi_L \cong \Psi_{soil} - (1/[K_r/A_L] + 1/[K_{sh}/A_L])E \tag{5.17}$$

Meristem growth and gas exchange are maximal when water stress is small, i.e., when Ψ_L is near zero. From Eq. (5.17) it can be seen that the advantage of high K_r/A_L and K_{sh}/A_L is that Ψ_L will be closer to Ψ_{soil}. Leaf-specific stem-segment conductivities, K_L, are high in adult pioneer trees, so the water potential drop from soil to leaf is much smaller than in old-forest species (Machado and Tyree 1994). This may promote rapid extension growth of meristems in pioneers compared with old-forest species. Also, stomatal conductance (g_s) and therefore net assimilation rate are reduced when Ψ_L is too low. During the first 60 days of growth of *Quercus rubra* L. seedlings, there was a strong correlation between midday g_s and leaf-specific plant conductance, $G=K_p/A_L$, where $K_p=K_rK_{sh}/(K_r+K_{sh})$ (Ren and Sucoff 1995). This suggests that whole-seedling hydraulic conductance is limiting g_s though its effect on Ψ_L. There also is reason to believe that whole-shoot conductance limits g_s in mature trees of *Acer saccharum* Marsh (Yang and Tyree 1993). Thus, high values of K_r/A_L and K_{sh}/A_L may promote both rapid extension growth and high net assimilation rates in pioneers.

Scaling is always necessary to normalize for plant size. As seedlings grow exponentially in size we would expect an approximately proportional increase in K_r and K_{sh}. Since roots and shoot both supply water to leaves and since an increase in leaf area means in increase in rate of water loss per plant, we would expect K_r and K_{sh} to be approximately proportional to A_L.

Tyree et al. (1998) studied the growth dynamics of root and shoot hydraulic conductance in seedlings of five neotropical tree species of contrasting ecological strategy. Two species were light-demanding pioneers and three were shade-tolerant forest species. All five species were grown under the same intermediate light regime. The pioneers versus shade-tolerant species had significantly higher growth rates in terms of the rate of increase in A_L, A_r, L, $TRDW$, K_r and K_{sh}. When the scaled root conductances were compared between species, no pattern was found relating K_r/A_r or K_r/L. On the other hand, all pioneers were significantly higher in terms of $K_r/TRDW$, K_r/A_L, $A_r/TRDW$, and $L/TRDW$. The tentative conclusion to be drawn from this rather limited study is that scaling by $TRDW$ or A_L may be of more ecological significance than scaling by L and A_r. Whenever possible, it is best to use all scaling methods in ecological and physiological studies of roots, but the less used scaling methods ($TWRD$ and A_L) are clearly important and could be used on their own.

The HPFM and RPP have recently been used to study ecological aspects of root physiology, e.g., the effect of drought and mycorrhizae on L_r. Readers interested in this aspect should consult Nardini et al. (2002).

5.8 Summary and Prospects

The main resistance to water uptake in root systems appears to be the radial resistance from the fine root surface to the stele. The next biggest resistance is the axial resistance in the first few cm of root length near the apex of the roots. The axial resistance is determined by the number and diameter of vessels in any given cross section. Since the vessels are fewer in number and smallest in diameter in the first 10 cm of maize roots, the axial resistance of the first 10 cm is about 180 times more than the next 10 cm. Hence most of the root resistance is in the apical 10 cm and most of that in the root radius.

Equations describing solute and water transport in roots must account for the coupling between flows of solute and water and for the non-ideality of the osmotic forces. Hence root water and solute transport require a minimum of three parameters, L_r (root hydraulic conductance), P_s (solute permeability), and σ (reflection coefficient). Some people believe that two L_r values are needed, one (L_{rp}) that describes the conductance to pressure-driven flow and the other (L_{ro}) that describes osmotic driven flow, which is ten times or more lower. In this chapter I argue against this concept and suggest instead that measurements of L_{ro} are incorrect. The differences between L_{rp} and L_{ro} could be explained by the time it takes solutes to reach the osmotic barrier in roots, i.e., the Casparian band. Others have reported that values of σ might vary with water flux rates in roots but I argue that these conclusions might also be in error because the erroneous measurements of σ did not take into account the likely coupling of solute flux to water flux.

More work needs to be done to fully elucidate the mechanism and pathway of water and solute flux in roots and the experimental approach needs to be extended to a wider range of root types. So far, maize roots are the most fully characterized roots, but it seems unlikely to me that maize roots can be taken as a universal model of all root systems. The second exciting area concerns the role of aquapores in root hydraulic conductivity and in periodicity. Unpublished results from roots of tobacco, peach, honey locust and apple have revealed a very strong diurnal periodicity in which roots are 10 times more conductive to water at midday than at midnight (Tyree and Zimmermann 2002). Our understanding of whole-plant water relations will have to be revised after further elucidation of the periodicity of root hydraulic conductivity, because up until recently we have all assumed that roots act like constant, passive pathways for water movement.

References

Esau K (1960) Anatomy of seed plants. Wiley, New York

Fiscus El (1975) The interaction between osmotic- and pressure-induced water flow in plant roots. Plant Physiol 55:917–922

Fiscus EL (1977) Determination of hydraulic and osmotic properties of soybean root systems. Plant Physiol 59:1013–1020

Frensch J, Hsiao TC, Steudle E (1996) Water and solute transport along developing maize roots. Planta 198:348–355

Kedem O, Katchalsky A, Curran PF (1962) Permeability of composite membranes. Parts 1, 2 and 3. Trans Faraday Soc 59:1918–1953

Lopushinsky W (1964) Effects of water movement on ion movement into the xylem of tomato roots. Plant Physiol 39:494–501

Machado J-L, Tyree MT (1994) Patterns of hydraulic architecture and water relations of two tropical canopy trees with contrasting leaf phenologies: *Ochroma pyramidale* and *Pseudobombax septenatum* Tree Physiol 14:219–240

Mees GC, Weatherley PE (1957) The mechanism of water absorption by roots. I. Preliminary studies on the effects of hydrostatic pressure gradients. Proc R Soc Lond Ser B 147: 367–380

Miller DM (1985) Studies of root function in *Zea mays*. III. Xylem sap composition at maximum root pressure provides evidence of active transport into the xylem and a measurement of the reflection coefficient of the root. Plant Physiol 77:162–167

Nardini A, Salleo S, Tyree MT (2002) Ecological aspects of water permeability in roots. In: Waisel Y, Eshel A, Kafkafi U (eds) Plant roots: the hidden half. Marcel Dekker, New York, pp 683–698

Newman EI (1973) Permeability to water of five herbaceous species. New Phytol 72:547–555

Peterson CA, Murrmann M, Steudle E (1993) Location of major barriers to water and ion movement in young roots of *Zea mays* L. Planta 190:127–136

Peterson CA, Steudle E (1993) Lateral hydraulic conductivity of early metaxylem vessels in *Zea mays* L. roots. Planta 189:288–297

Ren Z, Sucoff E (1995) Water movement through *Quercus rubra* L. Leaf water potential and conductance during polycyclic growth. Plant Cell Environ 18:447–453

Schneider H, Zhu JJ, Zimmermann U (1997) Xylem and cell turgor pressure probe measurements in intact roots of glycophytes: transpiration induces a change in the radial and cellular reflection coefficients. Plant Cell Environ 20:221–229

Siefritz F, Tyree MT, Lovisolo C, Schubert A, Kaldenhoff R (2002) PIP1 plasma membrane aquaporins in tobacco: From cellular effects to function in plants. Plant Cell 14:869–876

Steudle E (1994) Water transport in roots. Plant Soil 167:79–90

Steudle E (1993) Pressure probe techniques: basic principles and application to studies of water and solute relations at the cell, tissue, and organ level. In: Smith JAC, Griffith H (eds) Water deficits: plant responses from cell to community. Bios Scientific Publishers, Oxford, pp 5–36

Steudle E, Frensch J (1996) Water transport in plants: role of the apoplast. Plant Soil 187:67–79

Steudle E, Henzler T (1995) Water channels in plants: do basic concepts of water transport change? J Exp Bot 46:1067–1076

Steudle E, Peterson CA (1998) How does water get through roots? J Exp Bot 49:775–788

Steudle E, Murrmann M, Peterson CA (1993) Transport of water and solutes across maize roots modified by puncturing the endodermis. Further evidence for the composite transport model of the root. Plant Physiol 103:335–349

Steudle E, Oren R, Schulze E-D (1987) Water transport in maize roots. Plant Physiol 84:1220–1232

Tsuda M, Tyree MT (2000) Plant hydraulic conductance measured by the high pressure flow meter in crop plants. J Exp Bot 51:823–828

Tyree MT (1999) Water relations and hydraulic architecture. In: Pugnaire FI, Valladares F (eds) Handbook of functional ecology. Marcel Dekker, New York, pp 221–268

Tyree MT, Zimmermann MH (2002) Xylem structure and the ascent of sap, 2nd edn. Springer, Berlin Heidelberg New York

Tyree MT, Patiño S, Bennink J, Alexander J (1995) Dynamic measurement of root hydraulic conductance using a high-pressure flowmeter in the laboratory and field. J Exp Bot 46:83–94

Tyree MT, Yang S, Cruiziat P, Sinclair B (1994) Novel methods of measuring hydraulic conductivity of tree root systems and interpretation using AMAIZED. Plant Physiol 104:189–199

Tyree MT, Velez V, Dalling JW (1998) Growth dynamics of root and shoot hydraulic conductance in seedlings of five neotropical tree species: scaling to show possible adaptation to differing light regimes. Oecologia 114:293–298

van den Honert TH (1948) Water transport in plants as a catenary process. Disc Farad Soc 3:146–153

Yang Y, Tyree MT (1993) Hydraulic resistance in the shoots of *Acer saccharum* and its influence on leaf water potential and transpiration. Tree Physiol 12:231–242

Zhu JJ, Zimmermann U, Thürmer F, Haase A (1995) Xylem pressure response in maize roots subjected to osmotic stress: determination of radial reflection coefficients by use of the xylem pressure probe. Plant Cell Environ 18:906–912